Distinct Potentiation of L-Type Currents and Secretion by cAMP in Rat Chromaffin Cells

V. Carabelli,* A. Giancippoli,* P. Baldelli,* E. Carbone,* and A. R. Artalejo†
*Dipartimento di Neuroscienze, Unità di Ricerca, Instituto Nazionale Fisica della Materia, 10125 Turin, Italy; and †Departamento de Toxicología y Farmacología, Universidad Complutense, 28040 Madrid, Spain

ABSTRACT We have investigated the potentiating action of cAMP on L-currents of rat chromaffin cells and the corresponding increase of Ca^{2+}-evoked secretory responses with the aim of separating the action of cAMP on Ca^{2+} entry through L-channels and the downstream effects of cAMP/protein kinase A (PKA) on exocytosis. In ω-toxin-treated rat chromaffin cells, exposure to the permeable cAMP analog 8-(4-chlorophenylthio)-adenosine 3′,5′-monophosphate (pCPT-cAMP; 1 mM, 30 min) caused a moderate increase of Ca^{2+} charge carried through L-channels (19% in 10 mM Ca^{2+} at +10 mV) and a drastic potentiation of secretion (~100%), measured as membrane capacitance increments (ΔC). The apparent Ca^{2+} dependency of exocytosis increased with pCPT-cAMP and was accompanied by 83% enhancement of the readily releasable pool of vesicles with no significant change of the probability of release, as evaluated with paired-pulse stimulation protocols. pCPT-cAMP effects could be mimicked by stimulation of β_1-adrenoreceptors and reversed by the PKA inhibitor H89, suggesting strict PKA dependence. For short pulses to +10 mV (100 ms), potentiation of exocytosis by pCPT-cAMP was proportional to the quantity of charge entering the cell and occurred independently of whether L, N, or P/Q channels were blocked, suggesting that cAMP acts as a constant amplification factor for secretion regardless of the channel type carrying Ca^{2+}. Analysis of statistical variations among depolarization-induced capacitance increments indicates that pCPT-cAMP acts downstream of Ca^{2+} entry by almost doubling the mean size of unitary exocytic events, most likely as a consequence of an increased granule-to-granule rather than a granule-to-membrane fusion.

INTRODUCTION

In chromaffin cells, L-type Ca^{2+} channels represent the final target of multiple modulatory pathways (Carbone et al., 2001). We found evidence that L-channel activity in bovine chromaffin cells (BCCs) is quickly downmodulated by receptor-coupled G-proteins (Hernández-Guijo et al., 1999; Carabelli et al., 2001; Cesetti et al., 2003) or inhibited within a few minutes by a cGMP-dependent protein kinase G (Carabelli et al., 2002). In parallel to this, L-channel activity can be potentiated by intracellular cAMP elevations induced by addition of membrane-permeable cAMP analogs (Carabelli et al., 2001) or β_1-adrenoreceptor stimulation (Cesetti et al., 2003). In principle, all of these signaling pathways can up- or downregulate the exocytotic responses of chromaffin cells by either: *1*), controlling the quantity of Ca^{2+} entry through Ca^{2+} channels (Ulate et al., 2000; Powell et al., 2000); *2*), acting on the Ca^{2+} sensitivity of the late steps of secretion (Renström et al., 1997; Lim et al., 1997), *3*), affecting the dimension and probability of release of the readily releasable pool (RRP) of vesicles (Sakaba and Neher, 2001); or *4*), varying the size and shape of single-vesicle release events (Machado et al., 2001). A clarification of these issues is of extreme interest in chromaffin cells, because activation of second-messenger pathways have autocrine origins and form the basis for the autocontrol of catecholamine release during cell activity.

The effects of cAMP on secretion are quite heterogeneous. Some reports point to a dramatic increase of exocytosis after protein kinase (PK) A and PKC application, but the effects are either partially dependent (Ämmälä et al., 1994) or fully independent of Ca^{2+} (Koh et al., 2000). In contrast, other reports demonstrate that cAMP does not alter the Ca^{2+} sensitivity and amount of depolarization-evoked release (Tse and Lee, 2000). In chromaffin cells, the results are even more heterogeneous and contradictory. Some reports point to a marked increase of basal and stimulus-evoked secretion with cAMP, pituitary adenylate cyclase-activating polypeptide, or forskolin (Morita et al., 1987; Parramón et al., 1995; Przywara et al., 1996; Machado et al., 2001), whereas other groups draw the opposite conclusion (Baker et al., 1985; Gandía et al., 1997; Jorgensen et al., 2002). In some work, L-channels and membrane voltage are shown to play an exclusive role in the increase of stimulus-induced secretion by cAMP (Artalejo et al., 1994), whereas in others, the role of these components appears more limited or unnecessary (Doupnik and Pun, 1992; Parramón et al., 1995).

Given this wide spectrum of responses, our goal was that of clarifying the role of Ca^{2+} channels in the exocytotic response of rat chromaffin cells (RCCs) and identifying the macroscopic and elementary components of the depolarization-evoked exocytosis affected by cAMP. We show here that 8-(4-chlorophenylthio)-adenosine 3′,5′-monophosphate (pCPT-cAMP) increases both L-currents and secretion, but the L-current increase accounts for only 20% of the total secretory response. In particular, cAMP doubles the size of the RRP of vesicles and the mean size of unitary exocytic events without affecting the probability of release. The

Submitted February 17, 2003, and accepted for publication April 21, 2003.
Address reprint requests to Dr. Valentina Carabelli, Department of Neuroscience, Corso Raffaello 30, 10125 Turin, Italy. Tel.: +39-011-6707702; Fax: +39-011-6707708; E-mail: valentina.carabelli@unito.it.

0006-3495/03/08/1326/12 $2.00

potentiating effects of cAMP occur regardless of the channel type controlling Ca^{2+} entry and are mimicked by β_1-adrenoreceptor stimulation through a PKA-mediated pathway, suggesting the existence of an effective positive-feedback signaling mediated by cAMP/PKA, which controls the fast release of catecholamine during RCC activity.

MATERIALS AND METHODS

Isolation and culture of RCCs

Chromaffin cells were obtained from the adrenal glands of adult female Sprague-Dawley rats (200–300 g) sacrificed by cervical dislocation. All experiments were carried out in accordance with the guidelines established by the National Council on Animal Care and were approved by the local Animal Care Committee of Turin University. Cell isolation was achieved as previously described (Cesetti et al., 2003). Cells were plated in four-well plastic dishes pretreated with poly-L-ornithine (1 mg/ml) and laminin (5 μg/ml in L-15 carbonate), incubated at 37°C in a water-saturated atmosphere with 5% CO_2, and used within 2–6 days after plating. The culture medium contained DMEM supplemented with 10% fetal calf serum (Invitrogen, Grand Island, NY), 50 IU/ml penicillin, 50 μg/ml streptomycin, and 0.25% gentamycin.

Electrophysiological recordings

Electrophysiological recordings were performed with an EPC-9 patch-clamp amplifier using the PULSE software (HEKA Electronic, Lambrecht, Germany). Pipettes were obtained from thin Kimax borosilicate glass, purchased from Witz Scientific (Holland, OH) and fire-polished to obtain a final series resistance of 2–3 MΩ.

Ca^{2+} currents were measured with the perforated-patch technique and started after the access resistance decreased below 15 MΩ, which usually happened within 10 min after sealing (Rae et al., 1991). Ca^{2+} currents were sampled at 10 kHz and filtered at 2 kHz. The holding potential was fixed at −70 mV and step depolarizations (10–200 ms) were applied from −30 to +30 mV. For better isolating L-type channels, a 200-ms prepulse to −40 mV was applied before the test pulse (see Results). The quantity of charge Q was calculated as the time integral of the inward Ca^{2+} current. Given the presence of an early inward Na^+ current [no tetrodotoxin (TTX) was used], the limits for the current integration were fixed 3–4 ms after the beginning of the pulse once 80% of the Na^+ currents were decayed and excluding the tail currents. Tail currents were omitted from the analysis because of their small contribution to the overall current (<2%) and the difficulties in separating Ca^{2+} tail currents from capacitative artifacts.

Exocytosis was estimated by the membrane-capacitance increment (ΔC) evoked by the depolarizing step according to the Lindau-Neher technique implemented as the ''sine + dc'' feature of the PULSE lock-in module (Ulate et al., 2000). A sinusoidal wave function (1 kHz, ±25 mV amplitude) was superimposed on the holding potential. Capacitance increments were acquired by the high time-resolution PULSE data, and between-depolarization capacitance data were recorded at the low time resolution using the X-Chart plug-in module of the PULSE software. To determine ΔC values, membrane capacitance was first averaged over 50 ms preceding the depolarization to give a baseline value; this was subtracted to the value estimated after the depolarization averaged over a 400-ms window, excluding the first 50 ms to avoid contamination by nonsecretory capacitative transients. Experiments were performed at room temperature (22–24°C). Data are given as mean ± SE for n = number of cells. Statistical significance was calculated using Student's paired t-test, and P values <0.05 (*) were considered significant. The symbol ** indicates a P value <0.01. One-way ANOVA followed by the Fisher's least-significant difference test for multiple comparisons was used to determine statistical significance between group means >2.

Fast capacitative transients during step depolarizations were minimized online by the patch-clamp analog compensation. Currents were not corrected for leakage, and for this reason, cells with leak current >15 pA at holding potentials were excluded from the analysis, either in control or after cAMP treatment. Moreover, cAMP incubation did not increase the leakage current, thus excluding the possibility that additional $[Ca^{2+}]_i$ induced greater depolarization-evoked exocytosis.

Solutions

Perforated-patch recordings were performed with an extracellular control solution containing (in mM) 135 NaCl, 2.8 KCl, 10 $CaCl_2$, 2 $MgCl_2$, 20 glucose, and 10 HEPES (pH 7.4 with NaOH). TTX was not added to prevent slowdown of Na^+-channel gating kinetics (Horrigan and Bookman, 1994). pCPT-cAMP (1 mM), isoproterenol (1 μM), ICI 118,551 (0.1 μM), nifedipine (5 μM), 1-methyl-3-isobutylxanthine (IBMX, 20 μM), and forskolin (10 μM) were purchased from Sigma (St. Louis, MO) and used at the concentrations indicated. The protein kinase inhibitor H89, purchased from CN Biosciences (Darmstadt, Germany), was dissolved in distilled water and added to the external solution to reach a final concentration of 1 μM; cells were incubated at least 10 min with H89 before recording. The ω-conotoxin-GVIA (ω-CTx-GVIA) and ω-agatoxin-IVA (ω-Aga-IVA) were purchased from Peptide Institute (Osaka, Japan) and prepared to the final concentration as described elsewhere (Cesetti et al., 2003).

The perforated-patch configuration was obtained using amphotericin B (Sigma). Amphotericin B was dissolved in dimethyl sulfoxide (DMSO) and stocked at −20°C in aliquots of 50 mg/ml. The pipette-filling solution contained (in mM) 135 $CsMeSO_3$, 8 NaCl, 2 $MgCl_2$, 20 HEPES, and 50–100 μg/ml amphotericin B (pH 7.3 with CsOH). Fresh pipette solution was prepared every 2 h. To more easily seal the cells, the patch pipette was immersed for a few seconds in an internal solution without amphotericin B and then backfilled with the internal solution containing amphotericin B. After sealing, series resistance decreased gradually to reach values <15 MΩ within 10 min.

Series resistance was compensated by 80% and monitored throughout the experiment. Because the drugs applied to the external solution did not affect the liquid junction potential (LJP), the indicated voltages were not corrected for the LJP at the interface between the pipette solution (135 $CsMeSO_3$) and the bath (135 NaCl), which was −13 mV (Barry and Lynch, 1991). The estimated Donnan equilibrium potential between the cell interior and the pipette was below −2 mV. Thus, the voltage bias for the present measurements was between −13 and −15 mV. Compared to measurements with whole-cell clamp recordings in 10 mM Ca^{2+} in which LJP is not compensated, the voltage bias reduces to ~−10 mV (see Cesetti et al., 2003).

RESULTS

Contribution of L-currents to depolarization-evoked secretion in RCCs

In a first set of experiments, we measured the contribution of L-channels to the depolarization-evoked secretion in RCCs, which were incubated for 12 min with ω-CTx-GVIA (3.2 μM) and ω-Aga-IVA (2 μM) (see Methods). Using 10 mM external Ca^{2+} and stimulating the cells every 45 s with pulses of 100 ms to +10 mV (−70 mV holding potential), Ca^{2+} currents were stable for several minutes (~11 min) and evoked a constant secretory response, evaluated as the increment of membrane capacitance (ΔC) after the transient depolarization (Fig. 1, *A* and *B*). To limit the contribution of

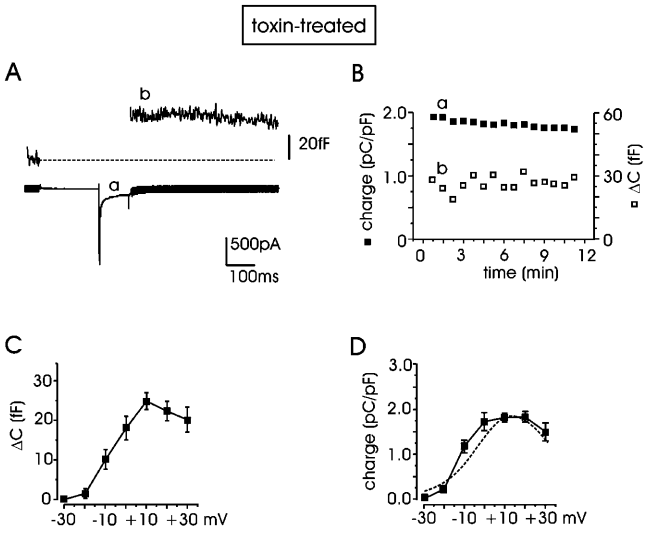

FIGURE 1 Stable exocytosis evoked by Ca^{2+} currents in RCCs. (*A*) Membrane capacitance increment (ΔC, *trace b*) evoked by Ca^{2+} influx (*trace a*) during depolarizing pulses recorded from a representative cell pretreated with ω-toxins (ω-CTx-GVIA, 3.2 μM and ω-Aga-IVA, 2 μM). Depolarizations to +10 mV (100 ms) were repeated every 45 s and preceded by a prepulse to −40 mV (see text). (*B*) Quantity of charge (■) and ΔC (□) plotted versus time for the experiment of panel *A*. The quantity of charge was normalized to the cell capacitance (in pC/pF) and evaluated as the time integral of the current during the test. Each point represents the quantity of charge measured during one depolarization; letters *a* and *b* indicate, respectively, the quantity of charge and capacitance increment shown in panel *A*. (*C*, *D*) Mean ΔC and mean quantity of charge measured during 100-ms depolarizations applied from −30 to +30 mV. In both cases, maximal responses peaked around +10 mV (n = 5–54 cells). The dashed curve is taken from Cesetti et al. (2003) and represents the I-V relationship of L-currents derived from the same cell preparation.

low-threshold T-type channels (Hollins and Ikeda, 1996) and non-L-channels expressed in RCCs (Gandía et al., 1995), a prepulse of 200 ms to −40 mV preceded the test pulse.

Under these experimental conditions (10 mM external Ca^{2+} and 100 ms pulse length), we first examined the contribution of N- and P/Q-type channels by comparing the mean quantity of Ca^{2+} charge density (in pC/pF) and the corresponding ΔC (in fF) values in control cells and in cells pretreated with the ω-toxins. We found that on average, the two toxins decreased by a comparable amount the mean charge density and the corresponding ΔC. Charge density decreased from 2.71 ± 0.29 (n = 38) to 1.84 ± 0.1 pC/pF (n = 54) while ΔC decreased from 32.8 ± 4.5 to 24.3 ± 2.1 fF (Fig. 2 *B*), suggesting that the ω-toxin-resistant currents (L + R) contribute 68 ± 11 and 74 ± 12% to the overall Ca^{2+} charge and exocytotic response, respectively. Notice that the contribution of the various Ca^{2+}-current components to the exocytotic response could be achieved because of the short pulses (100 ms), which were sufficiently long to induce enough secretion without saturating the RRP. Most likely, longer pulses (200–250 ms) would not have allowed the separation of the small contribution of N + P/Q currents from the predominant L + R component.

The contribution of L-channels was further estimated by adding nifedipine (5 μM) to the ω-toxin-treated cells (Fig. 2, *A* and *B*). In the presence of nifedipine, the mean charges and the corresponding ΔC values decreased to 0.58 ± 0.11 pC/pF and 10.4 ± 1.7 fF (n = 11), indicating that L-channels contribute to a large fraction of the ω-toxin-resistant currents and cell capacitance (68% and 57%, respectively). Successive perfusion with Cd^{2+} (200 μM) completely blocked the remaining current and secretion. Taken together, the data of Fig. 1, *A* and *B*, and Fig. 2 suggest that: 1), L-currents contribute predominantly to the total Ca^{2+} charge and exocytotic responses in RCCs (Gandía et al., 1995; Hernández-Guijo et al., 1999); 2), there is good proportionality between the quantity of charge entering the cell and the exocytotic response, regardless of the channel type carrying Ca^{2+} (Kim et al., 1995); and 3), ω-toxin-treated cells are characterized by a dominant L-current component and thus represent a suitable cell system for studying the potentiating effects of cAMP/PKA on L-currents and secretion (Cesetti et al., 2003). As shown in Fig. 1, *C* and *D*, the charge through ω-toxin-resistant channels and the corresponding ΔC started raising at −30 mV and reached their maximal amplitude at +10 mV. The voltage-dependence of Ca^{2+} charge in ω-toxin-treated cells (Fig. 1 *D*, *solid line*) overlapped nicely with the current-voltage relationship of L-currents derived

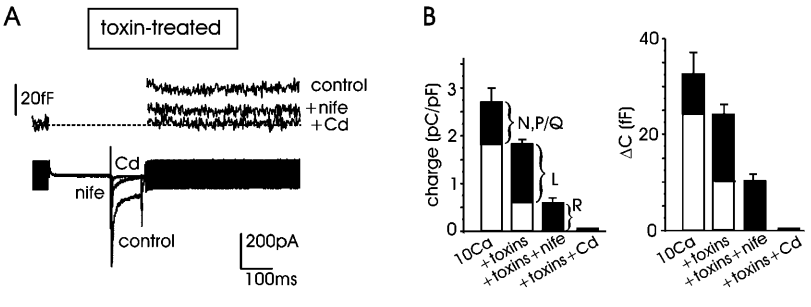

FIGURE 2 Calcium channel contribution to exocytosis in RCCs. (*A*) Ca^{2+} currents recorded at +10 mV after incubation with ω-toxins (control) and subsequent addition of 5 μM nifedipine to evaluate the contribution of R-channels. At the top are shown the corresponding ΔC variations. Residual Ca^{2+} current and exocytosis are suppressed by 200 μM Cd^{2+}. (*B*) Contribution of different channel types to Ca^{2+} charges (*left*) and exocytosis (*right*) evaluated using the same protocol of panel *A*. Mean quantity of charge and capacitance increment (ΔC) were measured in control (10 mM Ca^{2+}, ω-toxin-untreated cells), after toxin incubation (toxins), after toxins and addition of 5 μM nifedipine (toxins + nife), after toxins and 200 μM Cd^{2+} (toxins + Cd).

from the same cell preparation (Fig. 1 *D*, *dashed curve*; taken from Cesetti et al. (2003)).

Increasing intracellular cAMP potentiates Ca^{2+} currents and secretion by different degrees

Elevation of intracellular cAMP in BCCs (Carabelli et al., 2001) and stimulation of β_1-AR in RCCs (Cesetti et al., 2003) induce selective potentiation of L-type current through a PKA-mediated pathway. Given this, we tested whether the expected augmentation of L-currents by cAMP was paralleled by a comparable increase of exocytotic activity. We compared the Ca^{2+} currents and related secretion in groups of ω-toxin-treated cells, which were maintained in control conditions or exposed to the membrane-permeable cAMP analog pCPT-cAMP (1 mM, 30 min). In this latter group of cells, the cAMP analog was maintained at the same concentration in the bath during the measurements.

On average, by grouping data from cells of different animals and days in culture, the secretory responses measured at +10 mV increased from 24.3 ± 2.1 fF in control ($n = 54$) to 48.9 ± 3.9 fF for pCPT-cAMP-treated cells ($n = 25$) (101% increase; $P < 0.01$) (Fig. 3 *B*), whereas the quantity of charge carried through the mixture of L + R channels increased much less: from 1.84 ± 0.1 pC/pF to 2.2 ± 0.15 pC/pF (a 19.6% increase; $P < 0.05$). Similar increases in Ca^{2+} currents and ΔC values were estimated when cells of the same animal and day of culture were grouped together for statistical comparison (23% potentiation of Ca^{2+} charge and 95% increment of ΔC). Notice also that the Ca^{2+} charge increment induced by pCPT-cAMP (19–23%) is in good agreement with the 21% increase of Ca^{2+} current amplitude induced by β_1-AR stimulation on the same cell preparation (see Fig. 7 in Cesetti et al. (2003)). The charge increment is, however, much smaller than the increased single L-channel activity induced by cAMP in cell-attached patches in BCCs (80% increase of open probability at +20 mV; Carabelli et al., 2001). The reason for this is most likely attributable to the type of permeable ion (Ca^{2+} vs. Ba^{2+}) rather than to the cell type (bovine versus rat) used in the two sets of experiments. Replacing Ca^{2+} with Ba^{2+}, we could in fact observe that in RCC, cAMP increases Ca^{2+} current comparably with those reported in BCCs (not shown).

The action of pCPT-cAMP on secretion was also tested at various potentials and found that between 0 and +30 mV (Fig. 3 *C*), the potentiation was mainly voltage independent. Percentage of ΔC potentiation was 106%, 101%, and 82% at 0, +10, and +30 mV, respectively. The lower increase at −10 mV, in the region of maximal voltage sensitivity, is not statistically significant and may be simply due to a small shift of the ΔC versus voltage curve toward more positive potentials with cAMP.

cAMP alters the Ca^{2+} dependence of exocytosis

The Ca^{2+} dependence of exocytosis was evaluated by plotting ΔC values evoked by pulses of increasing duration (10–150 ms to +10 mV), versus the quantity of charge. For each pulse length, we measured the mean quantity of charge entering during the depolarization from control cells ($n = 19$) and from cells preincubated with pCPT-cAMP ($n = 20$). This mean value was used as the abscissa in the diagram of Fig. 4. Due to the short duration of the pulse, the dependence of exocytosis from the quantity of charge was sufficiently well fitted by a straight line for low Q values (<2.6 pC/pF).

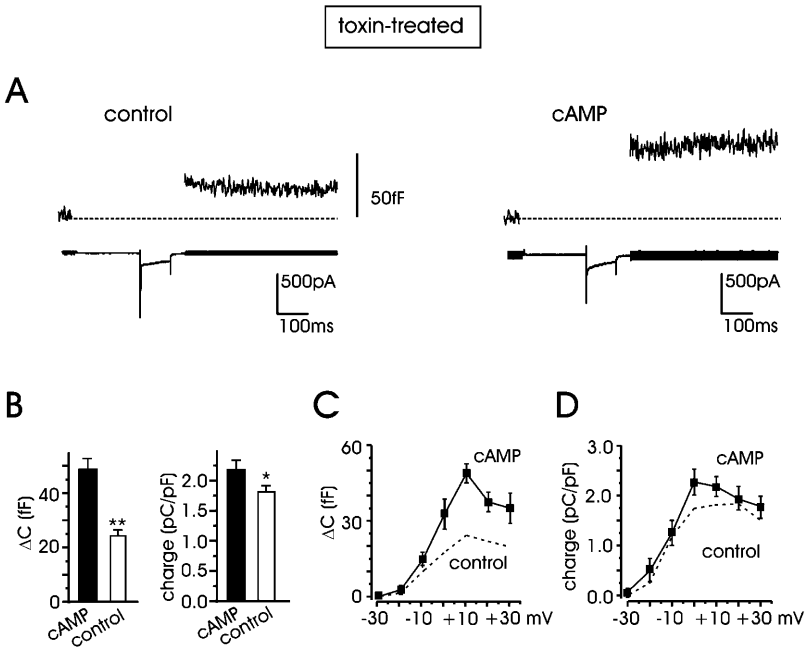

FIGURE 3 cAMP potentiation of L + R currents and exocytosis in toxin-treated cells. (*A*) Representative traces of ΔC variations and L + R currents measured at +10 mV in control cells (*left*), and after additional incubation with pCPT-cAMP (*right*). (*B*) Mean ΔC (*left*) and quantity of charge (*right*) averaged from $n = 54$ (control) and $n = 25$ (pCPT-cAMP) cells. (*C*) Depolarization-evoked exocytosis after cAMP treatment evaluated from −30 to +30 mV. The dashed line represents the ΔC increases in control conditions from Fig. 1 *C*. Depolarizations at the different potentials lasted 100 ms. (*D*) Quantity of charge versus potential after pCPT-cAMP incubation (*solid line*). The dashed line represents the control quantity of charge taken from Fig. 1 *D*.

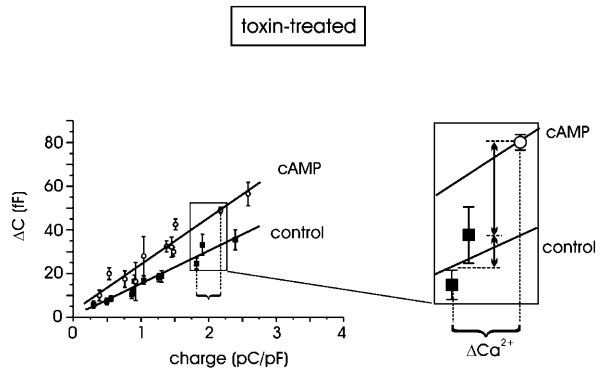

FIGURE 4 Calcium dependence of exocytosis in toxin-treated cells. Capacitance increments plotted versus the quantity of charge: each abscissa point is the mean charge value for the corresponding pulse length (from 10 to 150 ms). Standard errors on abscissas are omitted for clarity. In the range examined, ΔC data are positively correlated with the quantity of charge; linear regression for control and pCPT-cAMP-treated cells gave 15.1 ± 0.9 vs. 21.4 ± 1.7 fF/(pC/pF), respectively. Inset: see text for details.

Limited to this range, the regression analysis gave two significantly different slopes ($P < 0.01$) for control and pCPT-cAMP-treated cells: 15.1 ± 0.9 vs. 21.4 ± 1.7 fF/(pC/pF), respectively, confirming that the apparent sensitivity of vesicle fusion to Ca^{2+} ions is significantly potentiated by increasing the intracellular cAMP concentration. Indeed, a more rigorous approach would have required a fit of the ΔC vs. Q curve with polynomial functions with powers of 1.3–1.8 (Engisch and Nowycky, 1996), but our primary goal here was to compare the secretory responses in the two experimental conditions without any specific interest in the saturating exocytotic responses with longer pulses (see below, Fig. 6 *D*). Notice also that a straight-line fit of the ΔC vs. Q curve is also consistent with the data of Horrigan and Bookman (1994) for small values of Q in RCCs.

Fig. 4 allows a clear separation of the potentiating effects on secretion associated with the increased Ca^{2+} charges and the effects associated with the action of cAMP on the secretory apparatus. The inset shows clearly that a 20% increase of Ca^{2+} charges (ΔCa^{2+}) as induced by cAMP, would produce only a 25% increase of secretion in control cells (*small vertical arrow*), whereas the same ΔCa^{2+} produces a further 75% increase of secretion in cAMP-treated cells (*large vertical arrow*) to give a total increase of 100%. Thus pCPT-cAMP has a dual action on secretion: a minor one accounting for 25% of the total, which derives from the increased L-channel currents, and a larger one accounting for the remaining 75% due to an action of cAMP on the secretory apparatus downstream of Ca^{2+} entry.

cAMP-dependent potentiation of secretion occurs regardless of L-channels

Figs. 3 and 4 show clearly that cAMP potentiates L + R channels to a minor extent and depolarization-evoked secretion to a much larger one. Given that cAMP/PKA selectively potentiate the L-current component (Cesetti et al., 2003), our next goal was to investigate whether cAMP could preserve the same potentiating action on secretion after blocking the L-current. Therefore, we studied the effects of cAMP on nifedipine-resistant channels. Figs. 5, *A* and *B* show representative traces of current and secretion recorded in ω-toxin-untreated cells at +10 mV in 10 mM external Ca^{2+} plus 5 μM nifedipine (nife) and after exposure to pCPT-cAMP (nife + cAMP). On average, we found that Ca^{2+} influx through the nifedipine-resistant channels (R, N, and P/Q) was not significantly affected by pCPT-cAMP: mean quantity of charge was 0.92 ± 0.1 ($n = 16$) in control and 1.02 ± 0.2 pC/pF ($n = 12$) after pCPT-cAMP incubation ($P < 0.5$; Fig. 5 *B*). On the contrary, pCPT-cAMP potentiated secretion by 87%, increasing ΔC from 18.9 ± 2.4 to 35.4 ± 3.9 fF. Thus, in contrast with previous reports on bovine and calf chromaffin cells, in which the increased secretion induced by cAMP appears strictly associated with the presence or the recruitment of L-channels (Artalejo et al., 1994; Engisch and Nowycky, 1996), in RCCs, the main potentiating effect of cAMP on secretion is unrelated to these channels.

To further support this finding, we measured whether cAMP could similarly potentiate the depolarization-evoked exocytosis in ω-toxin-treated cells and in the presence of 5 μM nifedipine, i.e., when only the R-component was available. We found that the small secretory response in control conditions associated with the R-channels (10.4 fF, $n = 11$) increased by a factor of ~2 after incubation with pCPT-cAMP (21.2 fF, $n = 5$; Fig. 5, *C* and *D*) with no significant change of the R-current component (Fig. 5 *D*). Taken together, the results of Fig. 5, *B* and *D*, and Fig. 3 *B* suggest that the potentiating effects of cAMP are proportional to the amount of charge entry, regardless of the channel types carrying Ca^{2+}. This suggests that cAMP mainly acts on secretion as an amplification factor unrelated to a specific Ca^{2+} channel type, very likely at a site downstream of Ca^{2+} entry.

cAMP increases the size of the RRP without altering the probability of release

The net increase of membrane capacitance induced by cAMP may have different origins. cAMP may increase: 1), the size of the readily releasable pool of vesicles; 2), the fractional release of vesicles (probability of release, p); 3), the mean exocytic single-vesicle capacitance (Δc), or a combination of the three possibilities. To gain further insight into these mechanisms, we first estimated the maximal size of the readily releasable pool of vesicles and the fractional release by applying two consecutive depolarizing pulses and measuring the decline of ΔC after the first pulse (Gillis et al., 1996). The dual-pulse protocol was designed to elicit secretory depression (paired-pulse depression), taking care that

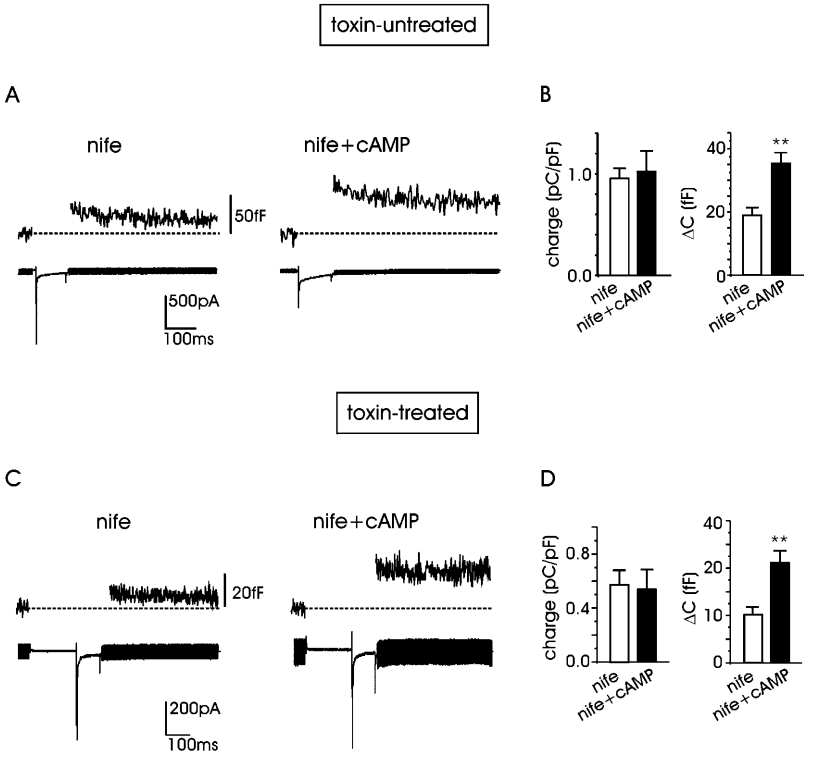

FIGURE 5 cAMP potentiates secretion without affecting Ca^{2+} entry through nifedipine-resistant channels. (*A*) Ca^{2+} current through nifedipine-resistant channels (N, P/Q, R) and corresponding exocytosis recorded from a toxin-untreated RCC in the presence of nifedipine (5 μM; *left*). Step depolarization to +10 mV. To the right, same protocol but the cell was incubated with pCPT-cAMP (1 mM). (*B*) pCPT-cAMP does not potentiate the quantity of charge through nifedipine-resistant channels at +10 mV, whereas it significantly upregulates capacitance increase ($P < 0.01$). (*C*) The effect of cAMP was evaluated on toxin-resistant R-channels (at +10 mV) and on the related secretion. Nifedipine was applied to block the L-channel contribution. (*D*) Mean quantity of charge of R-channels is not modified with pCPT-cAMP incubation, whereas exocytosis is significantly increased ($P < 0.01$).

the two Ca^{2+} injections applied in rapid succession were identical. For this reason, two depolarizations were set at 0 and +10 mV (100 ms). From the sum and the ratio of the two consecutive capacitance increases, ΔC_1 and ΔC_2 (Gillis et al., 1996), we estimated the maximum size of the RRP (Bmax) and the fractional release (p); the former from the equation $\text{Bmax} = (\Delta C_1 + \Delta C_2)/(1 - (\Delta C_2/\Delta C_1)^2)$ and the latter from $p = (1 - \Delta C_2/\Delta C_1)$.

Fig. 6 *A* shows Ca^{2+} current traces (L + R) and ΔC increases evoked by the dual-pulse protocol for one representative control and one pCPT-cAMP-treated cell, both previously incubated with ω-toxins (3.2 μM GVIA and 2 μM Aga IVA). Paired pulses were applied 45 s apart, repeated 3–5 times, and the ΔC_1 and ΔC_2 increases were monitored and averaged. Fig. 6 *B* summarizes the results obtained from 10 control cells and 16 cells pretreated with pCPT-cAMP. We found that in control conditions, the size of the RRP was estimated between 22.2 ± 1.3 fF (ΔC_1) and 35.2 ± 3.4 fF (Bmax). After incubation with pCPT-cAMP, the size of the RRP was significantly increased, varying between 35.2 ± 3.0 fF (ΔC_1) and 61.3 ± 6.5 fF (Bmax). Thus, by comparing the Bmax values from the two groups of cells, we estimated a 74% increase of the RRP. From the data of Fig. 6 *B* it is also evident that the ratio $\Delta C_2/\Delta C_1$, and thus the value of p, in control and pCPT-cAMP-treated cells is unchanged (0.32 ± 0.07, $n = 10$ in control vs. 0.37 ± 0.04, $n = 16$ with cAMP; $P < 0.5$; Fig. 6 *C*), indicating that the probability of release is preserved by cAMP exposures.

As shown by Horrigan and Bookman (1994) and Gillis et al. (1996), the size of the RRP can also be estimated by measuring the plateau value of ΔC after a series of pulses of increasing length, applied sequentially at sufficiently low rate to allow for pool refilling between pulses. Fig. 6 *D* shows that both at control (*filled squares*) and in the presence of cAMP (*open circles*) the capacitance increase reaches plateau values with pulse duration above 150 ms. With pulses of 10–200 ms to +10 mV, we found progressively larger secretory responses well fitted with an exponential function of comparable time constant (80.2 control and 83.5 ms cAMP) and maximal values of 40 fF in control and 73 fF for pCPT-cAMP-treated cells (83% increase). These findings are in good agreement with the RRPs estimated by the paired-pulse and with the time course of ΔC versus pulse duration derived by Horrigan and Bookman (1994) in RCCs. Notice also that the estimated RRP in control cells appears in good agreement with the value estimated for BCCs (34 fF; Gillis et al., 1996).

cAMP increases the size of single exocytic events

Chromaffin granules are too small to be resolved as individual fusion events in perforated-patch capacitance recordings (see Henkel and Almers, 1996). An alternative method for estimating the quantal size of individual exocytotic events is based on statistical analysis of trial-to-trial variations between depolarization-induced capacitance in-

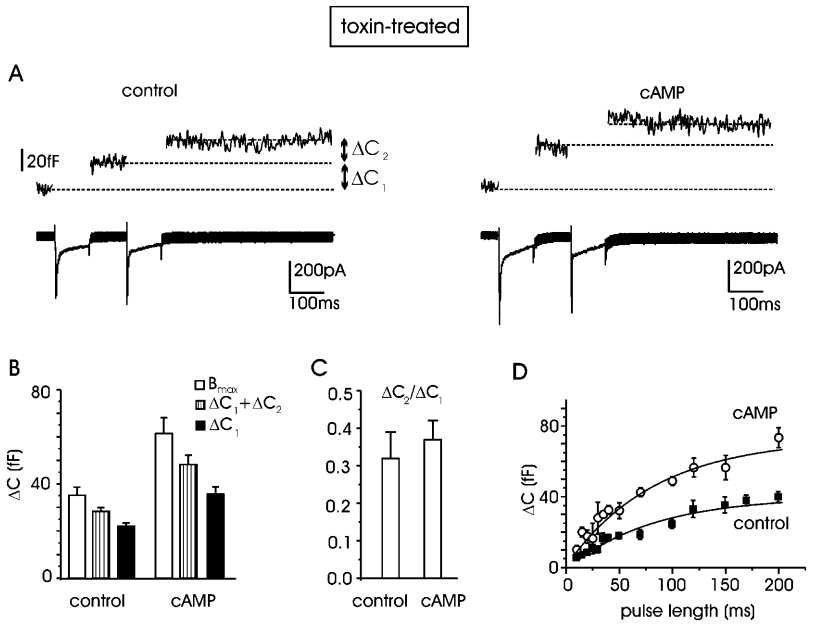

FIGURE 6 cAMP increases the size of the RRP of vesicles in toxin-treated cells. (*A*) The RRP is estimated by means of the double-pulse protocol (see text). Recordings from a control toxin-treated cell (*left*) and traces from a cell additionally incubated with 1 mM pCPT-cAMP (*right*) are shown. (*B*) Mean values of the maximum size of the RRP (Bmax, *open bars*) estimated from 10 control cells and 16 with cAMP. Striped bars represent the sum of the two membrane-capacitance increases ($\Delta C_1 + \Delta C_2$); solid bars indicate the mean ΔC_1 increase evoked by the first depolarization. (*C*) The mean ratio $\Delta C_2/\Delta C_1$ is summarized for control and cAMP-treated cells. (*D*) Plot of ΔC increases versus pulse duration for estimating the RRP size identified with the plateau value. Data points were fitted to the exponential function $y(x) = y_0\,(1 - \exp(-x/\tau))$. The parameters of the fit for control and cAMP-treated cells were, respectively, $y_0 = 40$ and 73 fF, $\tau = 80$ and 83 ms.

creases (Moser and Neher, 1997). Using this approach, we measured the ΔC increases after repetitive short depolarizations (20 ms) at +10 mV, applied at 0.3 Hz. Between 180 and 200 depolarizations were collected over a period of 9–10 min, and the corresponding ΔC values plotted versus time (Fig. 7 *A*). Because of a certain degree of rundown variability during high-frequency stimulation, an analysis bin of four neighboring ΔC values was used. The bin analysis moved forward point-to-point to calculate means and variances. Sample variances (σ^2) were then plotted versus the averaged sample means ($\langle \Delta C \rangle$) and fitted by a regression line. The slope of the linear regression gave the mean exocytic size (Δc) according to the equation: $\sigma^2 = \Delta c \times \langle \Delta C \rangle$ (Moser and Neher, 1997).

In the cell populations analyzed, there was a net increase of the variance in pCPT-cAMP-treated cells, compared to control, suggesting a net increment of Δc due to the action of cAMP. To show this more clearly, Fig. 7, A_1 and B_1 reports the time course of ΔC taken from two cells (control and pretreated with pCPT-cAMP) which started from comparable initial ΔC values (35 fF) and decayed to a similar stationary ΔC value (12 fF). The time course of the calculated σ^2 is given in Fig. 7, A_2 and B_2, where the net increase of σ^2 with cAMP despite the similar mean ΔC for most of the pulses (Fig. 7, A_1 and B_1, *solid curves*) is evident. The calculated Δc values were 0.9 in control and 2.3 fF with pCPT-cAMP (Fig. 7, A_3 and B_3) and on average, mean Δc values increased about twofold in cAMP-treated cells with respect to control cells (2.1 ± 0.3, $n = 9$ vs. 1.02 ± 0.07 fF, $n = 10$; $P < 0.01$; Fig. 7, A_3 *inset*), suggesting that pCPT-cAMP approximately doubles the size of elementary exocytic events. Notice that the increase of variance after cAMP exposure was evident during both the decaying part of the mean capacitance (nonstationary fluctuation) and the mean steady values at later times (stationary fluctuations). This is a good indication that our estimate of mean Δc is little or nonbiased by undesired fluctuations of the transient capacitance associated with Na^+-channel gating, which should remain unaltered with cAMP. In fact, cAMP does not affect the size of Na^+ currents. In four control cells and four cells treated with cAMP the estimated ratio of Δc ($\Delta c_{cAMP}/\Delta c_{control}$) calculated over 150 pulses during stationary conditions was in fact 2.05 ± 0.34.

cAMP-induced potentiation of exocytosis is mediated by PKA activation and mimicked by β_1-adrenergic stimulation

To establish whether an increase of cAMP could potentiate exocytosis through PKA activation, a group of cells ($n = 28$) was incubated with the PKA inhibitor H89 (1 μM). On average, H89 had no significant action on the quantity of charge through L + R channels (Fig. 8 *A*) and on the corresponding depolarization-evoked secretion, with respect to control (Fig. 8 *B*). In contrast, simultaneous incubation of H89 (1 μM) and pCPT-cAMP (0.5 mM) in 12 cells completely suppressed the pCPT-cAMP-induced potentiation of exocytosis and current ($P < 0.01$ and $P < 0.05$, respectively, with ANOVA). Similarly, we found that when the cAMP/PKA pathway was suppressed by H89, the size of the RRP (Bmax) became indistinguishable from control (Fig. 8 *C*), indicating that the action of cAMP on RRP is mediated by PKA.

Given that RCCs express sufficient densities of β_1-adrenoreceptors able to potentiate L-currents (Cesetti et al., 2003), this autocrine pathway could in principle increase the

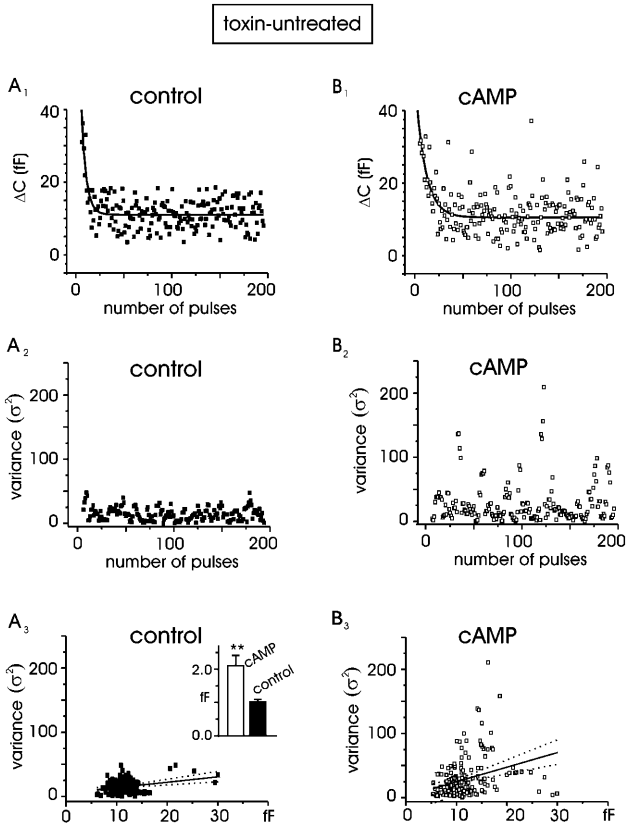

FIGURE 7 cAMP increases the single quantal size. Nonstationary statistical analysis of the secretory responses evoked by 20-ms depolarizations at +10 mV repeated at 0.3-Hz frequency for control (*A*) and pCPT-cAMP-treated (*B*) cells. (A_1, B_1) ΔC values measured in response to consecutive depolarizations for two representative cells. (A_2, B_2) Sample variances versus time calculated from panels A_1 and B_1. (A_3, B_3) Plot of variances versus the corresponding means. Linear regression (*solid line*) had a slope of 0.9 fF (control) and 2.3 fF (cAMP). Dotted lines represent the confidence limits of the fit (95%). Inset: mean quantal size for control ($n = 9$) and cAMP-treated cell ($n = 10$), $P < 0.01$.

endogenous levels of cAMP to values capable of potentiating vesicle exocytosis as well. Thus, we tested whether the selective β_1-AR stimulation could mimic the effects of pCPT-cAMP, using a solution containing the nonselective β-AR agonist isoproterenol (1 μM) and the specific β_2-AR antagonist ICI 118,551 (0.1 μM; Fig. 9 *A*).

In 10 cells incubated and perfused with the mixture isoproterenol + ICI 118,551, the mean quantity of charge measured at + 10 mV was 2.20 ± 0.19 pC/pF (Fig. 9 *B*), and the corresponding mean membrane capacitance increase was 39.6 ± 0.4 fF (Fig. 9 *D*). These capacitance values significantly differed from the controls ($P < 0.01$) but were statistically undistinguishable from those of pCPT-cAMP-treated cells ($P < 0.3$). In line with this, we found that exposures of RCCs to mixtures of the adenyl cyclase activator forskolin (10 μM) and the phosphodiesterase inhibitor IBMX (20 μM) could as well mimic the action of β_1-AR stimulation or exogenous cAMP (Fig. 9 *B*, $n = 12$). Thus, physiological stimulation of RCCs to produce endogenous cAMP via β_1-AR stimulation is shown to be as effective as elevating exogenous cAMP in producing a marked potentiation of depolarization-evoked secretion.

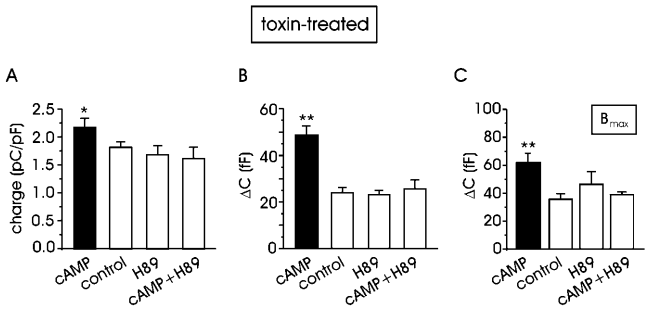

FIGURE 8 Potentiation of exocytosis in toxin-treated cells is mediated by PKA (*A*) Mean quantity of charge during 100-ms depolarization at +10 mV with the solutions indicated. In all cases, cells were previously incubated with toxins. Quantity of charge with pCPT-cAMP significantly differed from control, H89-treated cells, and those incubated with H89 + pCPT-cAMP ($P < 0.05$) (*B*) Mean ΔC increases in different experimental conditions. Statistical significance was $P < 0.01$. (*C*) The maximum size of the RRP estimated with the dual-pulse protocol. The secretory response with cAMP is statistically different from that of all the other groups ($P < 0.01$).

DISCUSSION

We have provided evidence that cell exposure to cAMP causes a potentiation of both the quantity of charge carried

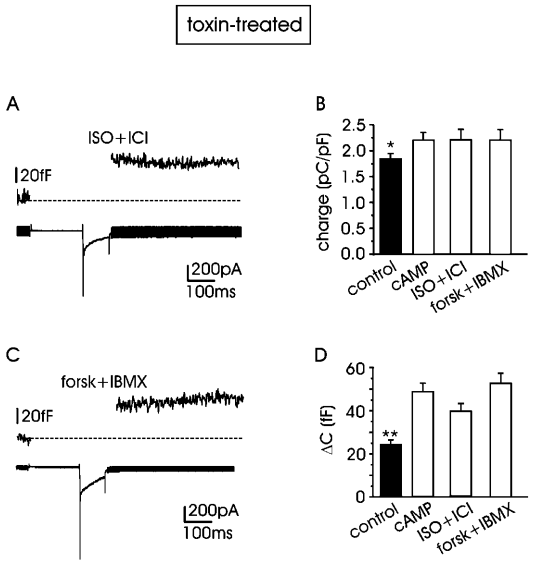

FIGURE 9 Selective β_1-adrenergic stimulation mimics the cAMP-induced potentiation of exocytosis in toxin-treated cells. Depolarization-evoked exocytosis and L + R currents recorded at +10 mV with external 10 mM Ca^{2+}, with isoprenaline (1 μM) + ICI 118,551 (0.1 μM) ($n = 10$) to selectively stimulate β_1-adrenoreceptors (*A*) or with the mixture of forskolin (10 μM) + IBMX (20 μM), $n = 12$ (*C*). Mean quantity of charges (*B*) and capacitance increment (*D*) in control and with the solutions indicated. Either increasing cAMP or stimulating β_1-AR causes both parameters (quantity of charge and capacitance increment) to differ significantly from control (*$P < 0.05$; **$P < 0.01$, respectively).

by Ca^{2+} channels and depolarization-evoked exocytosis measured through membrane-capacitance increases. We found that whereas the upregulation of Ca^{2+} charge by cAMP is specific for L-channels and causes a moderate increase of Ca^{2+} influx (19%), potentiation of exocytosis occurs independently of the availability of L-channels and causes a constant amplification by a factor of ~2 of the secretory response regardless of the channel types carrying the current (Fig. 3 *B* and Fig. 5, *B* and *D*). The increase of secretion is voltage independent in the range between 0 and +30 mV, i.e., at voltages in which inward Ca^{2+} currents are around their maximum (see Fig. 1 *D*) and action potentials span most of their overshoot (maximal spike amplitude, +40 mV). Thus, cAMP represents an effective modulator of neurotransmitter secretion that primarily amplifies Ca^{2+}-dependent exocytosis in RCCs without producing drastic increases of Ca^{2+} influx.

Our findings are in line with data of various groups showing that treatment with forskolin or cAMP analogs potentiates KCl-induced secretion from adrenal chromaffin cells and increases Ca^{2+} entry through L-channels in BCCs (Morita et al., 1987; Doupnik and Pun, 1992; Parramón et al., 1995; Przywara et al., 1996). Other groups draw opposite conclusions, showing inhibitory effects of cAMP (or forskolin) on nicotine-induced release (Baker et al., 1985; Cheek and Burgoyne, 1987) and either no effects or inhibition of Ca^{2+} currents in chromaffin cells (Gandía et al., 1997; Jorgensen et al., 2002). Such discrepancies may partially derive from the existence of complex modulatory pathways involving cAMP, nicotinic receptors, and Ca^{2+}-channel activation, and may also be partially associated with different experimental conditions of Ca^{2+}-current recordings. Indeed, the weak potentiating effects of cAMP and β_1-AR stimulation on L-channels (Cesetti et al., 2003) can be easily lost and hardly detected in internally dialyzed cells under whole-cell recording conditions (see Carbone et al., 2001).

Our findings also differ from those of other groups showing that potentiation of secretion by cAMP in calf chromaffin cells is fully associated with the voltage-dependent recruitment of ''facilitation'' L-channels (Artalejo et al., 1994). In the case of RCCs, elevation of cAMP produces only a partial increase of L-currents, and most of the increased secretion by cAMP is unrelated to Ca^{2+} entry through L-channels.

cAMP increases the size of the RRP and single secretory events

Our finding that short-term incubation with the cAMP analog causes an 83% increase in the size of RRP of vesicles is in line with fluorescence and ultramorphological studies showing increased vesicular transport in rat kidney cells (Muñiz et al., 1996) and number of functional release sites in cultured hippocampal neurons with cAMP (Kohara et al., 2001). Potentiation of RRP may imply either an increased vesicle population (Gillis et al., 1996), an increased size of secretory vesicles, or both. The results shown in Fig. 7 concerning the nonstationary fluctuation analysis of capacitance increases indicate that cAMP acts at the single-vesicle level by favoring a net increase in the size of single exocytic events, Δc, from 1.02 to 2.1 fF. These findings suggest two types of considerations. The first concerns the estimated value of Δc in control conditions, which appears in good agreement with previous measurements of mean quantal secretory events using patch-amperometry in RCCs ($\leq$1.25 fF; Tabares et al., 2001) and with the mean exocytic vesicle capacitance estimated in isolated mouse chromaffin cells using time-locked ΔC and amperometric current averages (1.28 fF; Moser and Neher, 1997). A value of 1–1.2 fF/vesicle sets an upper limit of 36 granules for the RRP in control conditions. This is about a factor of two larger than that estimated by Horrigan and Bookman (1994), which was based on the assumption that the mean Δc was ~2 fF.

The second consideration concerns the almost doubling of the mean size of individual secretory events with cAMP, which is in excellent agreement with recent amperometric measurements showing that cAMP (or forskolin) slows down the kinetics of single exocytotic spikes and increases by up to 50% the quantity of released catecholamines, without altering the frequency of secretory events (Machado et al., 2001). As indicated, the increased size of unitary exocytic events by cAMP may result from either the existence of a granule population with larger mean size due to preexocytotic granule-to-granule fusion or to the fusion of a subpopulation of larger granules containing more catecholamines. Our findings would support the first possibility, because RCCs and mouse chromaffin cells possess a rather homogeneous population of granules associated with the RRP (Moser and Neher, 1997; Tabares et al., 2001), and there is no evidence that cAMP selectively increases the secretory competence of larger granules as well as their probability of fusion. On the contrary, cAMP increases the mean size of elementary events without altering the rate of release (see Fig. 6 *C* and Machado et al., 2001).

An increased size of unitary exocytic events by cAMP is not a unique property of chromaffin cells. Clear evidence for a similar effect is reported for rat melanotrophs, in which cAMP nearly doubles the size of quantal release estimated by monitoring the whole-cell membrane capacitance (Sikdar et al., 1998). In rat corticotrophs, there are morphometric data supporting a role for cAMP in promoting granule-to-granule fusion rather than granule-to-membrane fusion (Cochilla et al., 2000). These observations imply the existence of proteins in the membrane of secretory granules whose phosphorylation facilitates the fusion to neighboring granules. A potential molecular target of PKA mediating the observed effects on secretion is Snapin, whose phosphorylation and overexpression in BCCs leads to an increased size of the exocytic burst elicited by flash photolysis of caged

Ca^{2+} (Chheda et al., 2001). Another protein potentially involved in the cAMP effects on secretion downstream of Ca^{2+} entry is cysteine string protein (Evans et al., 2001) whose phosphorylation by PKA causes the same slowing and broadening of single amperometric spikes reported in BCCs (Machado et al., 2001).

cAMP effects on basal $[Ca^{2+}]_i$

An interesting observation of our work concerns the increased Ca^{2+} sensitivity of exocytosis observed with cAMP (Fig. 4). Based on the present data, the increased Ca^{2+} sensitivity of secretion with cAMP may just be a consequence of the increased mean size of the elementary secretory events, which fully accounts for the doubling of the RRP occurring independently of the channel types carrying the current. Indeed, because we have not performed microfluorimetric $[Ca^{2+}]_i$ measurements, we cannot exclude the possibility that part of the cAMP-induced potentiation may derive from an increased basal $[Ca^{2+}]_i$ due to either Ca^{2+} flowing through cAMP-phosphorylated L-channels at rest or Ca^{2+} released from intracellular stores during the 30-min cAMP incubation before measurements. However, our data and several other reports speak against this possibility. First, $[Ca^{2+}]_i$ elevations induced by cAMP are mainly associated with external Ca^{2+} flowing through L-type channels in BCCs (Parramón et al., 1995). If this is valid also for RCCs, then $[Ca^{2+}]_i$ elevations induced by cAMP incubation are expected to be strongly attenuated during the 4–5-min period at −70 mV usually waited while accessing the patch-perforated recording conditions. Notice that in our experimental conditions (Fig. 1 *B*), a 45-s period at −70 mV was sufficient to recover most of the inactivated Ca^{2+} channels and to reestablish basal $[Ca^{2+}]_i$ after the depolarization-evoked Ca^{2+} entry as demonstrated by the steadily exocytotic responses obtained for long periods of time. In addition, cAMP did not produce any further increase in the continuously monitored holding/leakage current at −70 mV (<15 pA), thus excluding any nonspecific leak of Ca^{2+} in cAMP-treated cells. Second, the above conclusions are consistent with the observations that short applications of the cAMP-membrane-permeable analog 8-Br-cAMP (100 μM) is effective in producing exocytosis without altering $[Ca^{2+}]_i$ in single RCCs using fura-2 (Soares Lemos et al., 1997) and indo-1-microfluorimetry (Anderova et al., 1998). Moreover, forskolin is capable of potentiating the secretory response to nicotine and muscarine without increasing $[Ca^{2+}]_i$ levels in rat adrenal glands (Warashina, 1998). Noteworthy, applications of forskolin or pituitary adenylate cyclase-activating polypeptide in single RCCs produce secretion only in the presence of extracellular Ca^{2+} and with a latency of 5–7 s, characteristics of mechanisms mediated by cAMP/PKA-signaling pathways (Przywara et al., 1996). Thus, most of the present data agree with the idea that, when occurring, cAMP-mediated elevations of $[Ca^{2+}]_i$ in RCCs are mainly associated with extracellular Ca^{2+} passing through Ca^{2+} channels and not with Ca^{2+} released from intracellular stores. Finally, it should be also noticed that most of the potentiation of exocytosis by cAMP occurred independently of the type of Ca^{2+} channel blocked (Fig. 5), suggesting that the action of cAMP on Ca^{2+} entry plays a marginal role in the potentiation of exocytosis.

cAMP effects on secretion are PKA dependent and mimicked by β_1-AR stimulation

The effects of cAMP on regulated exocytosis are usually mediated by activation of PKA, but there are examples of PKA-independent actions (Ozaki et al., 2000). In pancreatic β-cells a PKA-independent pathway coexists with a PKA-dependent one. The former is active when exocytosis is fast (<80 ms) and triggered by single depolarizations, whereas the latter is slowly activated by repeated depolarizations (Renström et al., 1997). This does not seem to apply to RCCs in which the enhanced secretion by cAMP during short depolarizations is fully counteracted by the PKA inhibitor H89. A further possibility of a PKA-independent action on hyperpolarization-activated cation currents (I_h) as reported in crayfish neuromuscular synapses (Beaumont and Zucker, 2000), is rather unlikely because the Cs^+ ions included in the solution pipette should warrant an effective block of any available I_h in RCCs.

Because our interest was mainly directed toward the dual action of cAMP on Ca^{2+} channels and exocytosis, we checked for the existence of membrane receptors that could be autocrinally activated by released transmitters and associated with the production of cAMP/PKA. In agreement with recent findings (Cesetti et al., 2003), we observed that similarly to cAMP and forskolin, β_1-AR stimulation induces a moderate increase of L-currents and a marked potentiation of exocytosis (Fig. 9). This indicates that remote stimulation of cAMP production via β_1-ARs during prolonged cell activity may represent a functional pathway by which RCCs can autocrinally upregulate catecholamine secretion without dramatically increasing Ca^{2+} influx. The packed columnar arrangement of chromaffin cells in the adrenal gland and the high stocking of catecholamine molecules in single vesicles (~1 M; Albillos et al., 1997) would favor, in fact, the accumulation of a sufficient amount of secreted adrenaline and noradrenaline molecules in the surrounding media during cell activity. Under these conditions, the released catecholamine would trigger a positive-feedback loop involving β_1-AR activation, cAMP/PKA production, and enhanced secretion, which would rapidly lead to maximal release during sustained adrenal gland stimulation.

We are grateful to Drs. J. M. Hernández-Guijo and M. Novara for helpful discussions and Dr. C. Franchino for helping with cell cultures.

This work was supported by the Italian National Research Council (CNR grants 01.00443.ST97 and CNRG00D3F1), the Italian Ministry of Research

(MIUR grant 2001055324_006), and by the Cavalieri Ottolenghi Foundation (Turin, Italy).

REFERENCES

Albillos, A., G. Dernick, H. Horstmann, W. Almers, G. Alvarez de Toledo, and M. Lindau. 1997. The exocytotic event in chromaffin cells revealed by patch amperometry. *Nature*. 389:509–512.

Ämmälä, C., L. Eliasson, K. Bokvist, P. Berggren, R. E. Honkanen, A. Sjoholm, and P. Rorsman. 1994. Activation of protein kinases and inhibition of protein phosphatases play a central role in the regulation of exocytosis in mouse pancreatic β cells. *Proc. Natl. Acad. Sci. USA*. 91:4343–4347.

Anderova, M., A. D. Duchene, J. G. Barbara, and K. Takeda. 1998. Vasoactive intestinal peptide potentiates and directly stimulates catecholamine secretion from rat adrenal chromaffin cells. *Brain Res.* 809:97–106.

Artalejo, C. R., M. E. Adams, and A. P. Fox. 1994. Three types of Ca^{2+} channel trigger secretion with different efficacies in chromaffin cells. *Nature*. 367:72–76.

Baker, E. M., T. R. Cheek, and R. D. Burgoyne. 1985. Cyclic AMP inhibits secretion from bovine adrenal chromaffin cells evoked by carbamylcholine but not by high K^+. *Biochim. Biophys. Acta*. 846:388–393.

Barry, P. H. and J. W. Lynch. 1991. Liquid junction potentials and small cell effects in patch-clamp analysis. *J. Membr. Biol.* 121:101–117.

Beaumont, V. and R. S. Zucker. 2000. Enhancement of synaptic transmission by cyclic AMP modulation of presynaptic Ih channels. *Nat. Neurosci.* 3:133–141.

Carabelli, V., M. D'Ascenzo, E. Carbone, and C. Grassi. 2002. Nitric oxide inhibits neuroendocrine Ca(V)1 L-channel gating via cGMP-dependent protein kinase in cell-attached patches of bovine chromaffin cells. *J. Physiol.* 541:351–366.

Carabelli, V., J. M. Hernández-Guijo, P. Baldelli, and E. Carbone. 2001. Direct autocrine inhibition and cAMP-dependent potentiation of single L-type Ca^{2+} channels in bovine chromaffin cells. *J. Physiol.* 532:73–90.

Carbone, E., V. Carabelli, T. Cesetti, P. Baldelli, J. M. Hernández-Guijo, and L. Giusta. 2001. G-protein- and cAMP-dependent L-channel gating modulation: a manyfold system to control calcium entry in neurosecretory cells. *Pflügers Arch.* 442:801–813.

Cesetti, T., J. M. Hernández-Guijo, P. Baldelli, V. Carabelli, and E. Carbone. 2003. Opposite action of β1- and β2-adrenergic receptors on CaV1 L-channel current in rat adrenal chromaffin cells. *J. Neurosci.* 23:73–83.

Cheek, T. R. and R. D. Burgoyne. 1987. Cyclic AMP inhibits both nicotine-induced actin disassembly and catecholamine secretion from bovine adrenal chromaffin cells. *J. Biol. Chem.* 262:11663–11666.

Chheda, M. G., U. Ashery, P. Thakur, J. Rettig, and Z.-H. Sheng. 2001. Phosphorylation of Snapin by PKA modulates its interaction with the SNARE complex. *Nat. Cell Biol.* 3:331–338.

Cochilla, A. J., J. K. Angleson, and W. J. Betz. 2000. Differential regulation of granule-to-granule and granule-to-plasma membrane fusion during secretion from rat pituitary lactotrophs. *J. Cell Biol.* 150:839–848.

Doupnik, C. A. and R. Y. Pun. 1992. Cyclic AMP-dependent phosphorylation modifies the gating properties of L-type Ca^{2+} channels in bovine adrenal chromaffin cells. *Pflügers Arch.* 420:61–71.

Engisch, K. L. and M. C. Nowycky. 1996. Calcium dependence of large dense-cored vesicle exocytosis evoked by calcium influx in bovine adrenal chromaffin cells. *J. Neurosci.* 15:1359–1369.

Evans, G. J. O., M. C. Wilkinson, M. E. Graham, K. M. Turner, L. H. Chamberlain, R. D. Burgoyne, and A. Morgan. 2001. Phosphorylation of cysteine string protein by protein kinase A. *J. Biol. Chem.* 276:47877–47885.

Gandía, L., R. Borges, A. Albillos, and A. G. García. 1995. Multiple calcium channel subtypes in isolated rat chromaffin cells. *Pflügers Arch.* 430:55–63.

Gandía, L., M. L. Vitale, M. Villaroya, C. Ramírez-Lavergne, A. G. García, and J.-M. Trifaró. 1997. Differential aspects of forskolin and 1,9-dideoxy-forskolin on nicotinic receptor- and K^+-induced responses in chromaffin cells. *Eur. J. Pharmacol.* 329:189–199.

Gillis, K. D., R. Mossner, and E. Neher. 1996. Protein kinase C enhances exocytosis from chromaffin cells by increasing the size of the readily releasable pool of secretory granules. *Neuron.* 16:1209–1220.

Henkel, A. W. and W. Almers. 1996. Fast steps in exocytosis and endocytosis studied by capacitance measurements in endocrine cells. *Curr. Opin. Neurobiol.* 6:350–357.

Hernández-Guijo, J. M., V. Carabelli, L. Gandía, A. G. García, and E. Carbone. 1999. Voltage-independent autocrine modulation of L-type channels mediated by ATP, opioids and catecholamines in rat chromaffin cells. *Eur. J. Neurosci.* 11:3574–3584.

Hollins, B. and S. R. Ikeda. 1996. Inward currents underlying action potentials in rat adrenal chromaffin cells. *J. Neurophysiol.* 76:1195–1211.

Horrigan, F. T. and R. J. Bookman. 1994. Releasable pools and the kinetics of exocytosis in adrenal chromaffin cells. *Neuron*. 13:1119–1129.

Jorgensen, M. S., J. Liu, J. M. Adams, W. B. Titlow, and B. A. Jackson. 2002. Inhibition of voltage-gated Ca^{2+} current by PACAP in rat adrenal chromaffin cells. *Regul. Pept.* 103:59–65.

Kim, S. J., W. Lim, and J. Kim. 1995. Contribution of L- and N-type calcium currents to exocytosis in rat adrenal medullary chromaffin cells. *Brain Res.* 675:289–296.

Koh, D.-S., M. W. Moody, T. D. Nguyen, and B. Hille. 2000. Regulation of exocytosis by protein kinases and Ca^{2+} in pancreatic duct epithelial cells. *J. Gen. Physiol.* 116:507–519.

Kohara, K., A. Ogura, K. Akagawa, and K. Yamaguchi. 2001. Increase in number of functional release sites by cyclic AMP-dependent protein kinase in cultured neurons isolated from hippocampal dentate gyrus. *Neurosci. Res.* 41:79–88.

Lim, W., S. J. Kim, H. D. Yan, and J. Kim. 1997. Ca^{2+}-channel-dependent and -independent inhibition of exocytosis by extracellular ATP in voltage-clamped rat adrenal chromaffin cells. *Pflügers Arch.* 435:34–42.

Machado, J. D., A. Morales, J. F. Gómez, and R. Borges. 2001. cAMP modulates exocytotic kinetics and increases quantal size in chromaffin cells. *Mol. Pharmacol.* 60:514–520.

Morita, K., T. Dohi, S. Kitayama, Y. Koyama, and A. Tsujimoto. 1987. Stimulation-evoked Ca^{2+} fluxes in cultured bovine adrenal chromaffin cells are enhanced by forskolin. *J. Neurochem.* 48:248–252.

Moser, T. and E. Neher. 1997. Estimation of mean exocytotic vesicle capacitance in mouse adrenal chromaffin cells. *Proc. Natl. Acad. Sci. USA*. 94:6735–6740.

Muñiz, M., M. Alonso, J. Hidalgo, and A. Velasco. 1996. A regulatory role for cAMP-dependent protein kinase in protein traffic along the exocytic route. *J. Biol. Chem.* 271:30935–30941.

Ozaki, N., T. Shibasaki, Y. Kashima, T. Miki, K. Takahashi, H. Ueno, Y. Sunaga, H. Yano, Y. Matsuura, T. Iwanaga, Y. Takai, and S. Seino. 2000. cAMP-GEFII is a direct target of cAMP in regulated exocytosis. *Nat. Cell Biol.* 2:805–811.

Parramón, M., M. P. González, and M. J. Oset-Gasque. 1995. A reassessment of the modulatory role of cyclic AMP in catecholamine secretion by chromaffin cells. *Br. J. Pharmacol.* 114:517–523.

Powell, A. D., A. G. Teschemacher, and E. P. Seward. 2000. P_{2Y} purinoceptors inhibit exocytosis in adrenal chromaffin cells via modulation of voltage-operated calcium channels. *J. Neurosci.* 20:606–616.

Przywara, D. A., X. Guo, M. L. Angelilli, T. D. Wakade, and A. R. Wakade. 1996. A non-cholinergic transmitter, pituitary adenylate cyclase-activating polypeptide, utilizes a novel mechanism to evoke catecholamine secretion in rat adrenal chromaffin cells. *J. Biol. Chem.* 271:10545–10550.

Rae, J., K. Cooper, P. Gates, and M. Watsky. 1991. Low access resistance perforated patch recordings using amphotericin B. *J. Neurosci. Methods*. 37:15–26.

Renström, E., L. Eliasson, and P. Rorsman. 1997. Protein kinase A-dependent and -independent stimulation of exocytosis by cAMP in mouse pancreatic B-cells. *J. Physiol.* 502:105–118.

Sakaba, T. and E. Neher. 2001. Calmodulin mediates rapid recruitment of fast-releasing synaptic vesicles at a calyx-type synapse. *Neuron.* 32:1119–1131.

Sikdar, S. K., M. Kreft, and R. Zorec. 1998. Modulation of the unitary exocytic event amplitude by cAMP in rat melanotrophs. *J. Physiol.* 511:851–859.

Soares Lemos, V., B. Bucher, and K. Takeda. 1997. Neuropeptide Y modulates ATP-induced increases in internal calcium via the adenylate cyclase/protein kinase A system in a human neuroblastoma cell line. *Biochem. J.* 321:439–444.

Tabares, L., E. Alés, M. Lindau, and G. Alvarez de Toledo. 2001. Exocytosis of catecholamine (CA)-containing and CA-free granules in chromaffin cells. *J. Biol. Chem.* 276:39974–39979.

Tse, A. and A. K. Lee. 2000. Voltage-gated Ca^{2+} channel and intracellular Ca^{2+} release regulate exocytosis in identified rat corticotrophs. *J. Physiol.* 528:79–90.

Ulate, G., R. S. Scott, J. González, J. A. Gilabert, and A. R. Artalejo. 2000. Extracellular ATP regulates exocytosis by inhibiting multiple Ca^{2+} channel types in bovine chromaffin cells. *Pflügers Arch.* 439:304–314.

Warashina, A. 1998. Modulations of early and late secretory processes by activation of protein kinases in the rat adrenal medulla. *Biol. Signals Recept.* 7:307–320.